REMOTE SENSING INSTRUMENTATION FOR EARTH SYSTEM SCIENCE AT NASA/MARSHALL SPACE FLIGHT CENTER*

A. R. Guillory, R. J. Blakeslee, R. E. Hood, G. J. Jedlovec,

Observing Systems Branch/ES43
NASA/Marshall Space Flight Center
Huntsville, Alabama, USA

D. M. Mach,

Institute for Global Change Research and Education
Huntsville, Alabama, USA

J. Rothermel, and R. W. Spencer

Observing Systems Branch/ES43
NASA/Marshall Space Flight Center
Huntsville, Alabama, USA

ABSTRACT

NASA/Marshall Space Flight Center (MSFC) has played an active role in the development and application of airborne remote sensing instrumentation for Earth system science over the last 16 years. Several instruments have been developed. These instruments are designed to observe water vapor, precipitation, lightning and storm electrification, winds and aerosols. These instruments have been used in several field experiments, including the Cooperative Huntsville Meteorological Experiment (COHMEX), the Tropical Oceans Global Atmospheres Coupled Ocean-Atmosphere Response Experiment (TOGA COARE), and the Convection and Precipitation/Electrification (CaPE) experiment.

1.0 INTRODUCTION

The National Aeronautics and Space Adminstration's (NASA's) Marshall Space Flight Center (MSFC) is playing an active role in the development and application of airborne remote sensing instrumentation for Earth system science. Instruments that have been flown or will fly soon include the Multispectral Atmospheric Mapping Sensor (MAMS), the Advanced Microwave Precipitation Radiometer (AMPR), the Lightning Instrument Package (LIP), the Airborne Field Mill (ABFM) and the Multi-center Airborne Coherent Atmospheric Wind Sensor (MACAWS). These instruments are designed to observe water vapor, precipitation, lightning and storm electrification, winds and aerosols. These instruments have been used in several field experiments, including the Cooperative Huntsville Meteorological Experiment (COHMEX), the Tropical Oceans Global Atmospheres Coupled Ocean-

* Presented at the First International Airborne Remote Sensing Conference and Exhibition, Strasbourg, France, 11-15 September 1994.

Atmosphere Response Experiment (TOGA COARE), and the Convection and Precipitation/Electrification (CaPE) experiment. Future flights will be associated with the Global Energy and Water Cycle (GEWEX) Continental-Scale International Project (GCIP), the GEWEX Water Vapor Project (GVaP) as well as for the validation of Earth Observing System (EOS) instrumentation. This paper will describe each of these instruments and their respective science objectives and results.

2.1 Multispectral Atmospheric Mapping Sensor (MAMS)

NASA developed several aircraft sensors in the mid 1980's to verify data from new satellite sensors and to collect unique datasets that would serve to justify future space-based instruments on low-Earth and geostationary observation platforms. In 1985, MAMS was developed and flown to verify small-scale water vapor features observed in Visible Infrared Spin Scan Radiometer (VISSR) Atmospheric Sounder (VAS) imagery on the Geosynchronous Operational Environmental Satellites (GOES). This aircraft sensor provided a unique opportunity to independently verify single pixel variations observed in the VAS channels (Menzel et al., 1986). This verification continued for several years providing useful correlative measurements (Jedlovec et al., 1986b; Moeller et al., 1989).

2.1.1 Instrument Description

MAMS is a multispectral scanner that measures reflected radiation from the Earth's surface and clouds in eight visible and near infrared bands, and thermal emission from the earth's surface, clouds, and atmospheric constituents (primarily water vapor) in three of four available infrared bands (Table 1). The instrument is flown on a NASA ER-2 high-altitude aircraft at a nominal altitude of 20 km, and provides a horizontal ground resolution for each field-of-view of about 100 m at nadir. From this altitude, the width of the entire cross path field-of-view scanned by the sensor is roughly 37 km and provides detailed resolution of atmospheric and surface features across the swath width and along the aircraft flight track.

Table 1. MAMS Channel Configuration.

Visible		Infrared		
Channel	Wavelength (μm)	Channel	Central Wavelength (μm)	Bandwidth @50% response
1	0.42 - 0.45	9	3.73	3.47 - 3.86
2	0.45 - 0.52	10	6.54	6.28 - 6.98
3	0.52 - 0.60	11	11.12	10.55 - 12.24[1]
4	0.60 - 0.67	12	12.56	12.32 - 12.71
5	0.63 - 0.73			
6	0.69 - 0.83			
7	0.76 - 0.99			
8	0.83 - 1.05			

The MAMS design is based on that of other instruments developed by Daedalus Enterprises, Inc. for visible and infrared mapping. It shares the same scan head, digitizer, tape system, and supporting electronics as other Daedalus airborne scanners for the NASA ER-2. The difference lies in the spectrometer channels, particularly in the infrared region (Jedlovec et al., 1986a; Jedlovec et al., 1989). Four of the MAMS visible and near-infrared channels are similar to the first four channels of the Thematic Mapper (TM) on Landsat. Therefore, these channels can be used in similar applications.

MAMS is somewhat unique compared to other airborne scanners, since it provides some additional thermal infrared channels which have similarity to other satellite sensors. The infrared channels from MAMS have commonality with infrared channels on several U.S. weather satellites including those from the Advanced High Resolution Radiometer (AVHRR) and the Visible Infrared Spin Scan Radiometer (VISSR) Atmospheric Sounder (VAS), and the recently launched GOES-8 imager and sounder. There are also similarities to the infrared channels of METEOSAT. The single thermal channel of the Landsat Thematic Mapper and SPOT cover a broader spectral range than MAMS.

2.1.2 Applications

MAMS data has and is being used for numerous applications. The MAMS 6.5 micrometer channel has been used to map variations in upper tropospheric water vapor associated with a variety of atmospheric disturbances (Menzel et al., 1986; Jedlovec et al., 1986b). The split window channels at 11 and 12 μm allow surface temperature estimations and the determination of the total integrated water content (IWC) in a column of the atmosphere as discussed by Jedlovec (1987, 1990). The MAMS has also been used to study geomorphology along the Gulf of Mexico coast. Reflectances in the visible and near infrared channels of MAMS have been used to estimate suspended sediment concentrations, their source regions, and spatial distribution. Data from a series of flights before and after passage of weather systems have enhanced the understanding of the role that these systems play in producing geomorphic changes (Moeller et al., 1989). A time sequence of multispectral imagery along the coast of California was collected in October of 1989 to investigate the feasibility of determining ocean motions by tracking features in the water.

Most recently MAMS has been used to map mesoscale water vapor over east central Florida near Cape Canaveral (Guillory and Jedlovec, 1994). A case study moisture analysis was done on 6 August 1991. A sea-breeze front developed along the Florida coastline and propagated inland. IWC retrievals were made using the Physical Split Window (PSW) technique (Guillory et al., 1993). The first guess was chosen to be the 1500 UTC sounding from the Cape Canaveral Air Force Station. Figure 1 shows an analysis of the retrievals contoured over a composite of four of six flight legs on 6 August over the CaPE domain.

The sea-breeze front is marked by the northwest to southeast oriented line of cumulus clouds. The analysis depicts a moisture maximum of ~40-44 mm along the front, with a somewhat drier region behind it and a relatively moist enviroment ahead of it. The southernmost flight leg is perpendicular to the coast shows a subtle but significant gradient (~4 mm/10 km) just behind the front. A weaker gradient is present over the Merritt Island/Indian river region. Confirmation of many of the IWC features shown by MAMS was provided by the was provided by the University of Wyoming King Air aircraft flying along the line AB approximately one hour after the MAMS data were collected.

Figure 1. A composite of MAMS visible images with IWC (mm) contours superimposed for 6 August 1991 over the Cape Canaveral region of east central Florida.

2.2 Advanced Microwave Precipitation Radiometer (AMPR)

AMPR remotely senses passive microwave signatures of geophysical parameters from an airborne platform. The instrument is a low noise system which can provide multifrequency microwave imagery with high spatial and temporal resolution. AMPR data are collected at a combination of frequencies (10.7, 19.35, 37.1, and 85.5 GHz) unique to current NASA aircraft instrumentation. These frequencies are well suited to the study of rain cloud systems, but are also useful to studies of various ocean and land surface processes. Additionally, the aircraft information collected at these frequencies offer a rich database for satellite simulations of the current Defense Meteorological Satellite Program (DMSP) Special Sensor Microwave/Imager (SSM/I), the NASA Tropical Rainfall Measuring Mission (TRMM) Microwave Imager (TMI) scheduled for launch in 1997, and the Multifrequency Imaging Microwave Radiometer (MIMR) planned to fly aboard the Earth Observing System (EOS) PM-1 platform.

2.2.1 Instrument Description

AMPR is a total power scanning multifrequency passive radiometer. AMPR is composed of two adjacent antenna systems with one large scanning mirror accommodating both systems. One antenna system was designed to use a copy of the SSM/I feedhorn for the three higher frequencies. The second antenna system collects data at 10.7 GHz using a feedhorn designed by Georgia Tech Research Institute.

AMPR is currently configured to fly aboard a high altitude NASA ER-2 aircraft. The ground spatial resolution of the nadir footprint from the nominal aircraft altitude of 20 km is 0.6 km for the 85.5

GHz channel, 1.5 km for 37.1 GHz, and 2.8 km for both the 19.35 and 10.7 channels The AMPR calibrates with external cold and warm loads after every fourth data scan. A total calibration sequence or a total data scan are each performed in a three second time period. The AMPR scanner sweeps through a total 90° (+/- 45° from nadir) data scan collecting a sample for each channel every 1.8° for a total of 50 samples per channel. Based upon the nominal aircraft altitude and an aircraft speed of 200 m s^{-1}, this scan rate yields contiguous footprints for the 85.5 GHz channel within a 40 km wide swath. The other three channels are oversampled by the factors given in Table 2 which also lists other performance characteristics of the radiometer.

The alignment of the feedhorns is adjusted such that vertical polarization is received 45° to the left of nadir and horizontal is received 45° to the right of nadir. An equal mixture of vertical and horizontal polarizations is received at nadir. A more thorough discussion of the instrument may be found in Spencer et al. (1994).

Table 2. AMPR instrument characteristics

IF Frequency	3 dB Bandwidth	Mainbeam Beamwidth	Cross-Oversampling	Efficiency	Polarization
85.5 GHz	1400 Mhz	1.8°	1.0x	93.2%	1.4%
37.1 GHz	900 Mhz	4.2°	2.3x	98.8%	0.4%
19.35 GHz	240 Mhz	8.0°	4.4x	98.7%	1.6%
10.7 GHz	100 Mhz	8.0°	4.4x	97.8%	0.2%

2.2.2 Sampling Of Tropical Convection Data

AMPR sampled the deep cloud regions of developing tropical cyclone Oliver on 4 February, 1993 during TOGA COARE. At this time, AMPR operated with a warm bias offset between a calibration target and a scene target of the same blackbody temperature. This produced data uncertainties of 2 to 3 K for the warmer calibrated brightness temperatures (Tb) only. However, this offset affected all the channels and does not alter the relative relationship between channels.

Contour plots of 10.7 and 19.35 GHz Tb are presented in Figure 2 for one of these regions. These plots present a 7.5 minute segment of data (i.e., 150 scan lines) with the top of each plot corresponding to 18:05:20 UTC and the bottom corresponding to 18:12:50 UTC. These data represent radiometrically warm rain and cloud structures over a radiometrically cold ocean background. Note how the 10.7 GHz Tb maxima of 180 K in the upper portion of the plot corresponds well with a 19.35 GHz Tb maxima of 280 K. However, in the lower portions of the plots the regions of maxima and contour patterns in the 10.7 GHz data are not matched by the 19.35 GHz contours.

The scatterplot in Figure 3 represents the relationship of the 10.7 GHz frequency to the 19.35 GHz frequency for the entire 7.5 minute flight segment. The coolest Tb for both frequencies in Figure 2 depict the ocean surface. The split in data points at the intersection of the 140 K 10.7 GHz line and the 185 K 19.35 GHz line is due to the rotating polarization sampling technique employed by the AMPR which is most noticeable for a polarized ocean background. The warmer Tb are caused by the microwave

emissions of the cloud and rain system. For 19.35 GHz Tb less than 280 K, the 10.7 GHz and the 19.35 GHz observations are correlated although the data display as much as a 50 K spread of 19.35 GHz Tb for a given 10.7 GHz Tb. This spread is due mostly to differing drop size distributions (i.e., small raindrops, large raindrops, and/or nonprecipitating cloud water) at various locations in the overall cloud and rain system. Adler et al. (1991) have previously demonstrated the importance of cloud water to Tb-rain relations using a three-dimensional cloud model-microwave radiative transfer model to simulate a tropical rainfall system.

In Figure 3, the 19.35 GHz Tb data appears to saturate at 280 K. At this given Tb, the 10.7 GHz data exhibits variations of 50 K. This corresponds to heavier (> 15 mm h^{-1}) rain rates to which the 19 GHz channel is not sensitive. For 10.7 GHz Tb greater than 260 K, Figure 2 also shows the 19.35 GHz data decreasing slightly to Tb between 270 K and 280 K. This is due to some scattering by larger raindrops and ice particles.

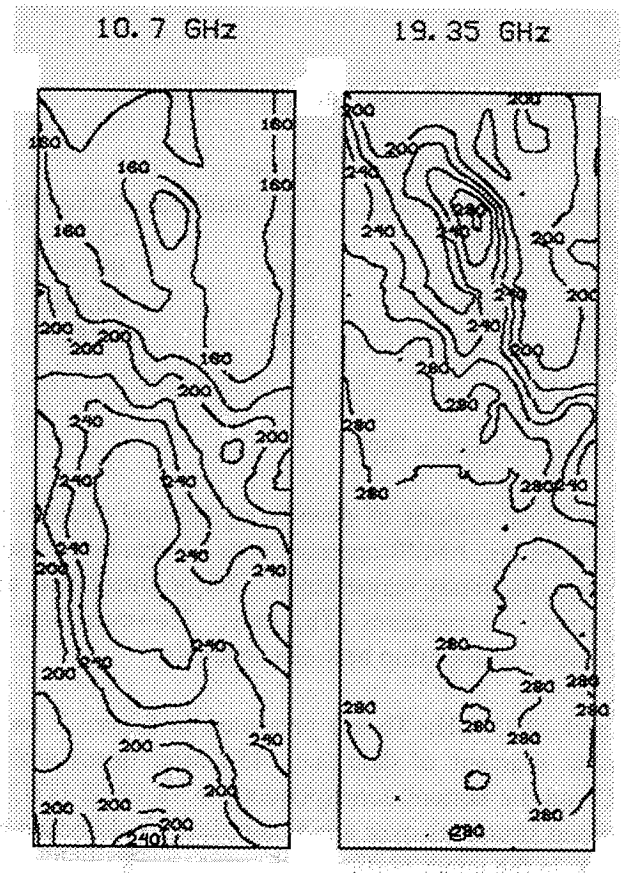

Figure 2. 10.7 GHz and 19.35 GHz Tb (K) contour plots of 4 February, 1993 AMPR data collected during TOGA COARE. The time at the top of the plot is 18:05:20 UTC. The time at the bottom of the plot is 18:12:50 UTC.

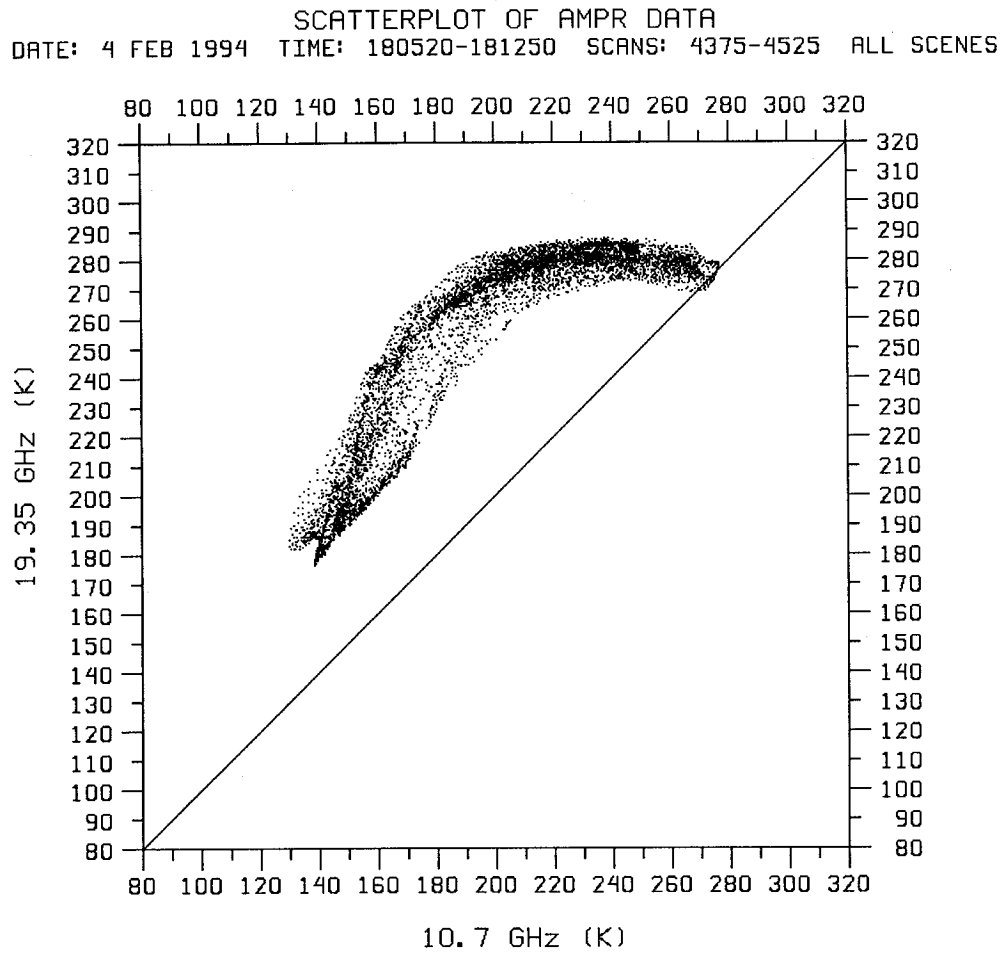

Figure 3. Scatterplot of 19.35 GHz and 10.7 GHz Tb (K) for the sequence of AMPR data presented in Figure 2.

2.3 Lightning Instrument Package (LIP)

The primary objective of LIP is to use aircraft platforms (ER-2, DC-8), multi-parameter datasets, and modeling studies to investigate relationships between lightning and storm electrification and a number of underlying and interrelated phenomena including the structure, dynamics, and evolution of thunderstorms and thunderstorm systems, precipitation distribution and amounts, atmospheric chemistry processes, and the global electric circuit (Blakeslee et al., 1989; Christian et al., 1983; Davis et al., 1983). This research is motivated by the desire to develop an understanding needed for the effective utilization and interpretation of data from the Optical Transient Detector (OTD), Lightning Imaging Sensor (LIS), and other satellite-based lightning detectors planned for the late 1990's and early 2000's (Christian et al., 1989; Christian et al., 1992). These satellite lightning detection systems will be characterized by high detection efficiencies (i.e., 90%) and the capability to detect both intracloud and cloud-to-ground

discharges during day and night. LIS is being developed by NASA for the Tropical Rainfall Measuring Mission (TRMM) satellite. OTD is a LIS prototype scheduled for launch in late 1994.

In support of this research, Lightning Instrument Packages (LIP's) have been developed for both the ER-2 and DC-8 aircraft. The ER-2 aircraft provides the best means to fly above thunderstorms since the ER-2 can be vectored over regions of interest. The ER-2 platform also provides a cloud top perspective similar to that viewed by a space sensor, albeit much closer. The DC-8 provides the capability for in-situ storm measurements. The aircraft instrumentation can detect total storm lightning and differentiate between intracloud and cloud-to-ground discharges. In addition, the instrumentation generally is flown with other sensor systems (e.g., infrared, passive microwave, radar, etc.) to provide new understanding of thunderstorms and precipitation and support detailed satellite simulations of storm measurements through the acquisition and analysis of multi-parameter datasets. By developing and maintaining the capability to monitor lightning and thunderstorms with the ER-2, NASA will also be able to provide important ground truth verifications and calibrations when OTD, LIS and other lightning detectors begin operations.

In the aircraft and related investigations, the emphasis is on establishing quantitative relationships and developing practical algorithms that employ lightning data, such as could be derived from satellite observations of optical lightning emissions. It is hoped that as a result of these kinds of investigations, lightning data alone and/or in conjunction with other remote sensing techniques will provide quantitative information about such storm characteristics as the occurrence and location of embedded convection, the strengths of updrafts and downdrafts, thermodynamic and electrical energy budgets, precipitation amounts and distributions, and the storm type, dimensions, and life cycle. Lightning rates, distribution, and characteristics (i.e., number of strokes per flash, ratio of intracloud to cloud-to-ground lightning, discharge energy, etc.) are all factors that may prove useful in devising quantitative algorithms.

2.3.1 Instrumentation

The ER-2 LIP consists of two electric field mills, conductivity probe, and data system. One of the field mills is installed on the upper Q-bay hatch cover and the second one is mounted on the aft section of the AMPR faring. The conductivity probe is integrated on the right hand superpod nose cone. The ER-2 LIP data system is mounted in a 19" vertical rack located in the aft portion of the ER-2 Q-bay. The ER-2 electric field mills measure components of the electric field (E_X, E_Z) over a dynamic range exceeding 3 orders of magnitude (i.e., there are 3 gain channels, x1, x46 and x2116). Hence, fair weather electric fields as well as large thunderstorm fields (e.g., 10-20 kV/m) are measured. Total lightning (i.e., cloud-to-ground, intracloud) is determined from electric field changes in the data. These data, particularly in conjunction with the DC-8 electric field measurements, provide information on the electrical structure of the thunderstorms encountered. The field mills also provide a measure of the electric charge on the aircraft. The conductivity probe measures the air conductivity at the aircraft altitude. The conductivity probe consists of a pair of Gerdien capacitor type sensors so that contributions due to positive and negative ions are obtained simultaneously. Storm electric currents are derived using the electric field and air conductivity measurements.

The DC-8 LIP consists of 4 electric field mills, a lightning location detector (i.e., a 3M Stormscope), and associated data system. The electric field mills measure the vector electric field (E_X, E_Y, E_Z) over a dynamic range from less than 1 V/m to over 10^6 V/m. Again, fair weather electric fields as well as large thunderstorm fields are obtained and abrupt electric field changes are used to identify lightning discharges (flash type and characteristics, storm lightning activity, etc.). The 3M Stormscope is a lightning direction finder that detects lightning sferics, obtains a bearing to the discharge, and estimates

the distance. The 3M Stormscope detects lightning out to about 200 nautical miles from the aircraft. In addition, a high voltage "stinger" is employed on the DC-8 to aid in obtaining an absolute calibration. The stinger is a device that allows the aircraft to be charged to a high known voltage in order to more accurately determine the field mill response to electric fields. The stinger is only operated a few times under fair weather conditions during a field program.

All LIP data is continuously recorded throughout the duration of each mission. The electric field and conductivity measurements are recorded on hard disk using PC-based data systems. Following each mission the data is archived on 8mm Exabyte tape. The Stormscope data is recorded on a Video Cassette Recorder (VCR). On some missions the aircraft dataset are complemented by lightning measurements from a ground-based lightning location network.

2.3.2 Applications

In January and February 1993, science flights were conducted during the TOGA COARE experiment to investigate electrical processes of tropical maritime convection and support multi-sensor precipitation algorithm development. The initial analysis of the data identified 117 overflights of electrified storms during 11 missions. Lightning was observed in only 23 of the storm overpasses (i.e., 19%). Generally, the storms overflown showed fairly weak electrical development, with the more intense storms having flash rates of only 1-2 discharges per minute. Figure 4 shows the horizontal (along the flight path) and vertical electric fields measured with the ER-2 LIP above a thunderstorm on 23 February 1993. Whenever electric fields were observed, depressed brightness temperatures in the 85 GHz channel of the AMPR indicated the presence of ice particles in the storm. However, small brightness temperature depressions in the 37 GHz channel were consistent with the weak electric fields and low lightning rates observed.

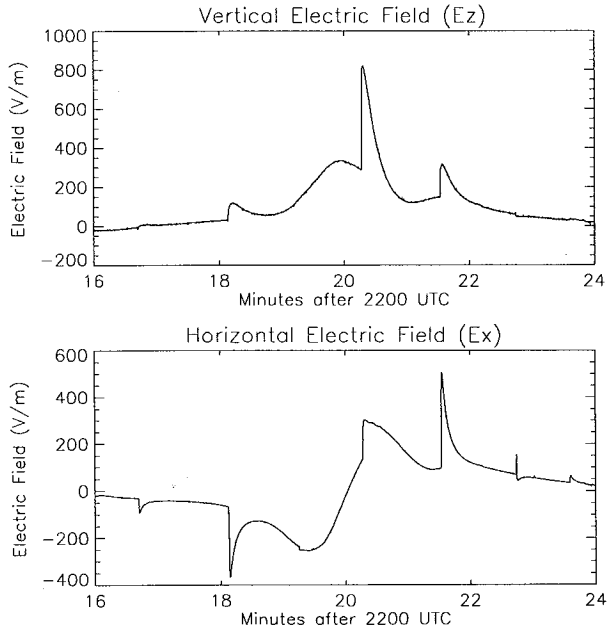

Figure 4. Example of electric fields measured with the ER-2 LIP.

2.4 Airborne Field Mill (ABFM)

The goal of the ABFM Project was to study the weather conditions that may lead to triggered lightning with an instrumented aircraft so that the spacecraft Launch Commit Criteria (LCC) rules for Cape Canaveral, Florida could be improved to increase launch availability without increasing launch risks. With a proposed shuttle and expendable launch rate of more than 40 per year, delays and cancellations due to the lightning related rules could become a significant factor in the launch schedule.

2.4.1 Instrument Description

The most critical component of the ABFM project was the set of aircraft field mills. The mills must have a dynamic range to sense the fair weather electric field under the presence of aircraft charge while at the same time be able to record the electric fields present near thunderstorms. Each mill has four separate output gains available at all times with full scale field values ranging from 2.3 kV m^{-1} to over 1 MV m^{-1}. Measurements of laboratory sensitivity values for the field mills ranged from 0.3 V m^{-1} for the most sensitive gain to 161 V m^{-1} for the least sensitive gain. The dynamic range and sensitivity of these mills allowed field mill calibrations under fair weather conditions while at the same time not saturating under thunderstorm electric field conditions. Five mills were mounted on the aircraft, four around the center of the body, and one in the tail as seen in Figure 5.

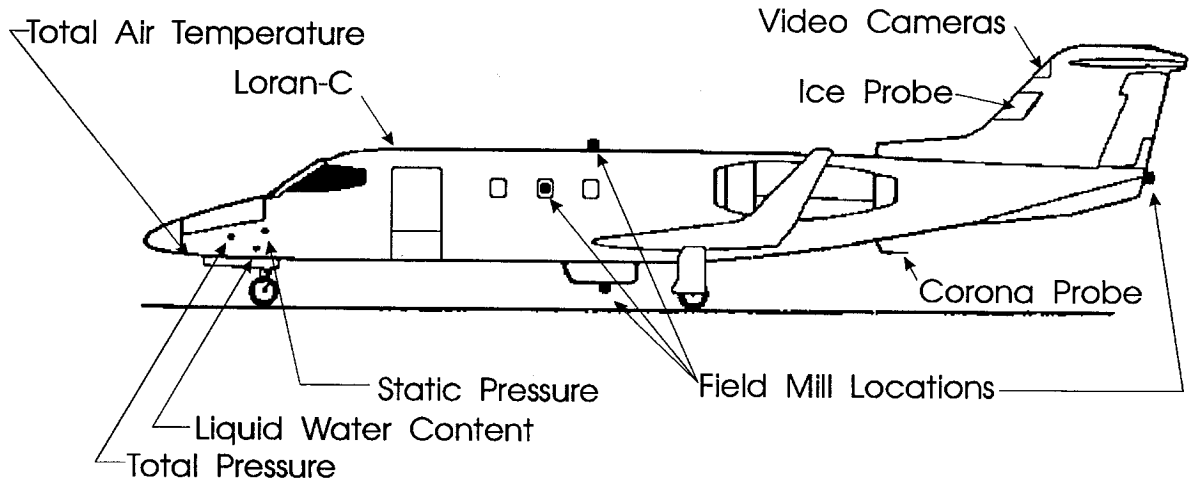

Figure 5. Diagram of ABFM aircraft showing locations of the electric field mills and other instrumentation used in the ABFM analysis.

The aircraft was a NASA Lear 28/29 and it was instrumented with the field mills and other equipment including a pressure altitude sensor, air speed indicator, and an X-band weather radar. Other meteorological instruments on the aircraft included an ambient temperature probe, a King Probe for liquid water content measurements, and a charge patch for rough estimates of atmospheric ice content. To aid in

field mill form factor calibrations, a +/-20 kV power supply attached to an external stinger was also installed.

The aircraft was also equipped with a LORAN-C navigation system. With transmission of all aircraft data to a ground system, the aircraft was tracked in real-time and guided to targets.

2.4.2 Kennedy Space Center (KSC) Resources

Data flights were made in the vicinity of KSC to take advantage of the available KSC/Air Force weather radar, ground field mills, instrumented towers, and a cloud-to-ground lightning locating system. The cloud-to-ground lightning system (Krider, 1988) located both positive and negative ground strikes to within a few kilometers in and around the KSC area. The ground-based field mills were part of the Launch Pad Warning System (LPWS) (Boyd et al., 1988). The mills have a frequency response of 10 Hz and are digitized at a rate of 50 samples per second. The tower data was part of the Weather Information Network Display System (WINDS), and consisted of wind speed and variability, wind direction and variability, and temperature and dew point at various heights from towers in KSC. The radar was a 5 cm WSR-74 located at Patrick Air Force Base (PAFB) located nearby.

2.4.3 Target Weather Conditions

The data collection concentrated on cloud systems and LCC rules which had the greatest chance of impacting launch availability and had the greatest potential of improving the LCC rules. Based on these goals, a general list of study targets based on LCC requirements and inputs from the NASA/Air Force personnel responsible for the ABFM project was produced. The list included, in rough priority order, 1) layered clouds, 2) rain clouds, 3) thunderstorm debris clouds, 4) cumulus clouds over the ocean, 5) cumulus clouds over land, and 6) cumulonimbus clouds.

2.4.4 Data Summary

There were a total of four deployments, two winter and two summer with 105 aircraft flights. Several areas where the LCC rules could be improved were found. The results from the analysis will be discussed in relation to the LCC rules.

Findings indicate that the current rules dealing with layered and rain clouds were not optimum. Although the layered and rain cloud LCC rules were never unsafe, they prohibited launches under many conditions where the electric fields aloft were benign. During the 863 penetrations of layered and rain clouds, only 15% of the fields aloft were significant. During 78% of the penetrations, however, no significant fields were found aloft yet the layered and rain cloud rules were violated. All of these would be false alarms, prohibiting launch when there was no electrical hazard aloft. It is clear from the analysis that a radar-based rule would better indicate significant fields aloft during layered/rain clouds conditions. An example radar-based rule that was proposed would reduced the false alarm rate from 78% to 23% while still maintaining the same margin of safety as the current rules. MSFC researchers are currently working with the NASA/Air Force launch community to refine and better define a new layered and rain cloud rule based on ABFM data.

The current rules prohibit launch vehicle penetration of debris clouds for three hours after the cloud becomes a debris cloud. The analysis shows that the electric fields in the debris clouds decay much sooner than three hours. The time is more on the order of one hour. Figure 6 shows debris cloud data. Note that all measured electric fields were less than 3 kV/m after one hour. Work is continuing with the NASA/Air Force launch community to determine a safe rule change that will not increase the risk from debris clouds.

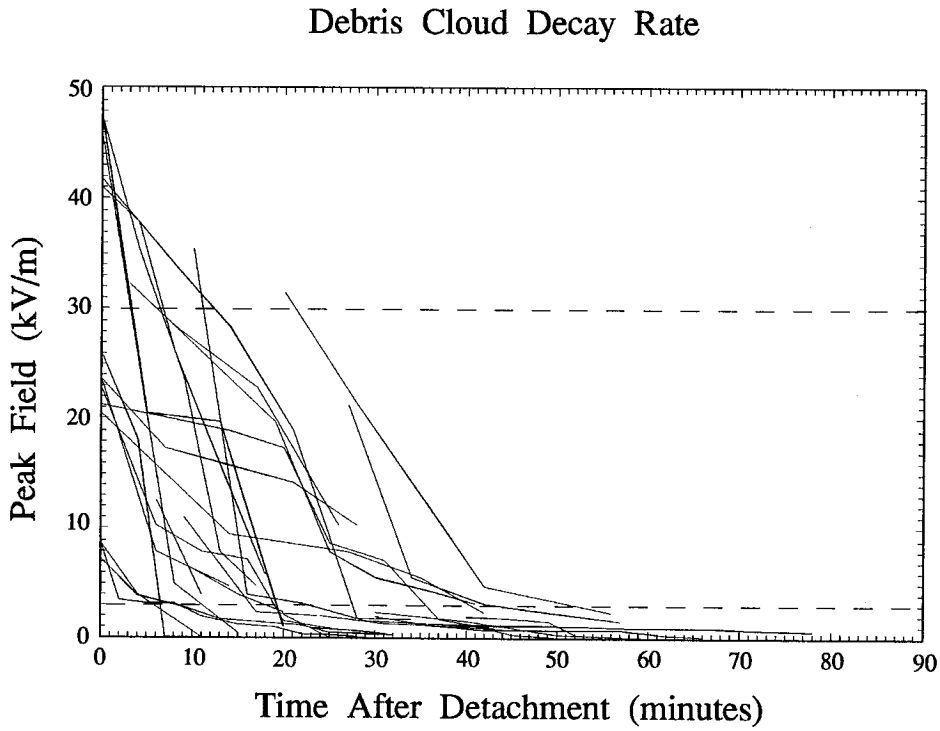

Figure 6. Electric field decay after the formation of debris clouds. The electric fields were determined from repeated penetrations of the debris cloud after their formation by the ABFM aircraft.

Current LCC rules do not allow launch vehicle penetration into clouds that have tops above the +5°C level. No significant electric fields were found in clouds that were nearly to the -10°C level. In addition, the ground based field mill system (LPWS) successfully indicated any clouds that developed significant electric fields. Findings show that once the cloud top exceeded the -10°C level, the electrification of the cloud was rapid and often severe. Based on ABFM data, one change to the LCC pertaining to the cumulus/cumulonimbus rule is being worked through the system while others are being studied to ensure launch safety in the very rapid development cases.

Improvements to some of the LCC rules have been made with our initial analysis. Further analysis of the large database will continue to improve the NASA/Air Force LCC rules. Some of the promising areas include further improvement in the cumulus/cumulonimbus rules, a relaxing of the debris cloud rules, and a total overhaul of the layered and rain cloud rules.

2.5 Multi-center Airborne Coherent Atmospheric Wind Sensor (MACAWS)

In Spring 1995, MACAWS will be put into operation for the first time. MACAWS is an airborne scanning pulsed CO_2 Doppler lidar capable of multi-dimensional wind and calibrated aerosol backscatter measurement from the NASA DC-8 research aircraft. Since Spring 1992, MACAWS has been under joint development by the lidar remote sensing groups of the MSFC, National Oceanic and Atmospheric Administration Environmental Technology Laboratory, and Jet Propulsion Laboratory. MSFC has lead responsibility for overall coordination, science definition, and mission planning. To minimize costs, each organization is sharing major hardware components and subsystems which, in nearly all instances, have been used in previous ground-based or airborne applications. The principal of operation is similar to that successfully employed by MSFC in previous airborne lidar experiments (Bilbro et al. 1986), although significant improvements to performance are being made (Rothermel et al. 1993). A pulsed lidar beam is generated and precisely directed using a scanning device mounted on the interior left side of the aircraft. The backscattered, Doppler-shifted radiation is measured to infer the line-of-sight wind velocity, assuming the aerosol scattering particles act as passive wind tracers. By scanning the lidar beam slightly forward and aft (co-planar scanning), a field of two-dimensional, ground-relative wind estimates is obtained within the scan plane (Fig. 7). Multiple scan planes, revealing the three-dimensional structure of the velocity and aerosol backscatter, are obtained by appropriately varying the scanner settings during flight (Fig. 8).

Following aircraft integration and check-flights, MACAWS will make an initial series of flights over the eastern Pacific and western U.S. using NASA Ames Research Center as a base of operations. The first objective is to improve understanding of atmospheric dynamic processes over critical scales of motion within the boundary layer and free troposphere, which are not routinely accessible with existing instrumentation. The goal is to apply these measurements toward improving parameterization schemes for sub-grid scale processes represented within climate and general circulation numerical models. At the same time, MACAWS observations will contribute toward improved understanding of specific mesoscale, or subgrid-scale, processes and features such as marine and continental boundary layer exchange, flow over complex terrain, and organized large eddies such as mesoscale cellular convection.

The second research objective is to investigate issues related to the performance of proposed, small-satellite Doppler lidar for measuring global tropospheric wind fields. Observations in this regard relate to design and performance simulation studies already underway at MSFC and affiliated organizations. MACAWS will be used to duplicate the perspective from space, thereby providing unique information not present in ground-based lidar observations. For example, satellite Doppler lidar data will contain a surface return signal applicable to calibration, atmospheric extinction estimation, and "ground-truth" velocity estimates. This information can be used to minimize velocity biases. Airborne studies with MACAWS will also provide guidance for improving signal processing algorithms. Other satellite Doppler lidar performance issues that will be addressed include: impact of spatial variability on velocity and backscatter sampling, detailed cloud properties, Doppler estimation near aerosol gradients, and long-term monitoring of natural surfaces that may serve as potential calibration targets for backscatter estimation as well as for monitoring instrument health. MACAWS may also serve to validate post-launch performance of satellite Doppler wind lidar as well. Participation is planned in multi-agency field

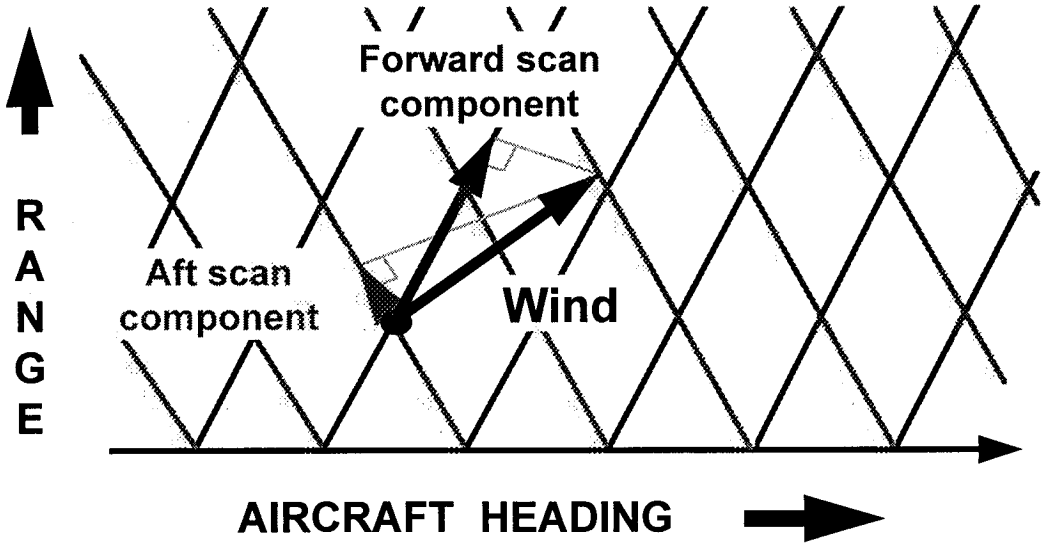

Fig. 7. Co-planar scan method for deriving 2-D wind measurements using line-of-sight lidar velocity.

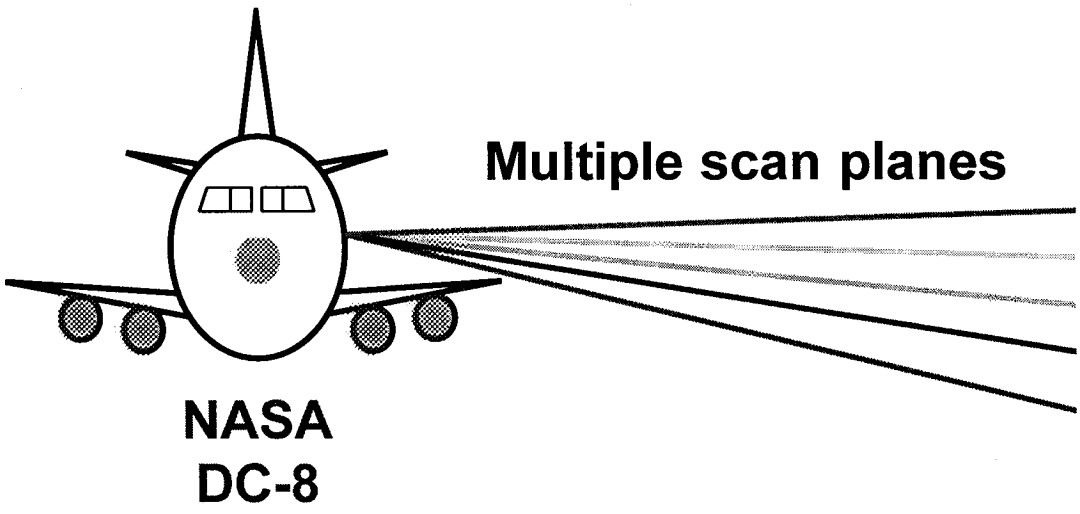

Fig. 8. Method for obtaining 3-D coverage of wind measurements by generating multiple 2-D scan planes.

programs addressing the understanding of the global energy and water cycle, as well as validation of satellite sensors planned for operation in 1996 and beyond.

3.0 SUMMARY

NASA/Marshall Space Flight Center (MSFC) is playing an active role in the development and application of airborne remote sensing instrumentation for Earth system science. Instruments that have been flown include the Multispectral Atmospheric Mapping Sensor (MAMS), the Advanced Microwave Precipitation Radiometer (AMPR), the Lightning Instrument Package (LIP), the Airborne Field Mill (ABFM). The Multi-center Airborne Coherent Atmospheric Wind Sensor (MACAWS) will begin flights in 1995. These instruments are designed to observe water vapor, precipitation, lightning and storm electrification, winds and aerosols. These instruments have been used in several field experiments, including the Cooperative Huntsville Meteorological Experiment (COHMEX), the Tropical Oceans Global Atmospheres Coupled Ocean-Atmosphere Response Experiment (TOGA COARE), and the Convection and Precipitation/Electrification (CaPE) experiment. Future flights will be associated with the Global Energy and Water Cycle (GEWEX) Continental-Scale International Project (GCIP), the GEWEX Water Vapor Project (GVaP) as well as for the validation of Earth Observing System (EOS) instrumentation.

4.0 REFERENCES

Adler, R.F., H.M. Yeh, N. Prasad, W.-K. Tao, and J. Simpson, "Microwave Simulations Of A Tropical Rainfall System With A Three-Dimensional Cloud Model."*J. Appl. Meteor.*, Vol. 30, No. 7, pp. 924-953, July 1991.

Bilbro, J.W., C.A. DiMarzio, D.E. Fitzjarrald, S.C. Johnson and W.D. Jones, "Airborne Doppler Lidar Measurements," *Appl. Opt.*, Vol. 25, No. 21, pp. 3952-3960, November 1986.

Blakeslee, R.J., H.J. Christian, B. Vonnegut, "Electric measurements over thunderstorms", *J. Geophys. Res.*, Vol. 94, pp. 13135-13140, 1989.

Boyd, B. F., A. F. Dye, and T. R. Strange, "Air Weather Service Support To Space Operations At The Eastern Test Range/Kennedy Space Center", AIAA-88-0282, AIAA 26th Aerospace Sciences Meeting, Reno Nevada , pp. 14.14-14.23, January 11-14, 1988.

Christian, H.J., R.J. Blakeslee, and S.J. Goodman, *Lightning Imaging Sensor (LIS) For The Earth Observing System, NASA TM-4350*, Marshall Space Flight Center, Huntsville, AL, pp. 44, 1992.

Christian, H.J., R.J. Blakeslee, and S.J. Goodman, "The Detection Of Lightning From Geostationary Orbit", *J. Geophy. Res.*, Vol. 94, pp. 13329-13337, 1989.

Christian, H.J. R.L. Frost, P.H. Gillaspy, S.J. Goodman, O.H. Vaughan, Jr., M. Brook, B. Vonnegut, and R.E. Orville, Observations Of Optical Lightning Emissions From Aove Thunderstorms Using U-2 Aircraft, *Bull. Am. Met. Soc.*, Vol. 64, pp. 120-123, February 1983.

Davis, M.H., M. Brook, H.J. Christian, B.G. Heikes, R.E. Orville, C.G. Park, R.G. Roble, and B. Vonnegut, " Some Scientific Objective Of A Satellite-Borne Lightning Mapper", *Bull. Am. Met. Soc.*, Vol. 64, pp. 114 - 119, February 1983.

Guillory, A. R., G. J. Jedlovec, and H.E. Fuelberg, "A Technique for Deriving Column-Integrated Water Content Using VAS Split-Window Data," *J. Appl. Meteor.*, Vol. 32, No. 7. pp. 1226-1241, July 1993.

Guillory, A. R. , and G. J. Jedlovec, "A Mesoscale Moisture Analysis of a Florida Sea Breeze From CaPE," Preprints, Conf. on Mesoscale Processes, Portland , Oregon, in press, July 17-22, 1994.

Jedlovec, G. J., *Determination Of Atmospheric Moisture Structure From High Resolution Mams Radiance Data.* Ph.D. Dissertation, Meteorology Department, The University of Wisconsin-Madison, pp. 173, 1987.

_____, "Precipitable Water Estimation From High Resolution Split Window Radiance Measurements". *J. Appl. Meteor.*, Vol. 29, No. 9, pp. 863-877, September 1990.

_____, K. B. Batson, R. J. Atkinson, C. C. Moeller, W. P. Menzel, and M. W. James, *Improved Capabilities Of The Multispectral Atmospheric Mapping Sensor (MAMS).* NASA TM-100352, Marshall Space Flight Center, Huntsville, Alabama, pp. 80, 1989.

_____, W. P. Menzel, R. Atkinson, G. S. Wilson, and J. Arveson, *The Multispectral Atmospheric Mapping Sensor (MAMS): Instrument Description, Calibration, and Data Quality.* NASA TM-86565, Marshall Space Flight Center, Huntsville, Alabama, pp. 37, 1986a.

_____, W. P. Menzel, G. S. Wilson, and R. J. Atkinson, "Detection Of Mountain Induced Mesoscale Wave Structures With High Resolution Moisture Imagery." *Second Conference on Satellite Meteorology/Remote Sensing and Applications*, Williamsburg, VA, pp. 365-369, May 13-16, 1986b.

Krider, E. P., "Spatial Distribution Of Lightning Strikes To Ground During Small Thunderstorms In Florida." Proceedings of t the 1988 Int. Aerospace and Ground Conf. on Lightning and Static Electricity, Oklahoma City, Oklahoma , pp. 318 - 323, April 19-22, 1988.

Menzel, W. P., G. J. Jedlovec, and G. S. Wilson, "Verification Of Small Scale Features In VAS Imagery Using High Resolution MAMS Imagery". *Second Conference on Satellite Meteorology/Remote Sensing and Applications*, Williamsburg, VA, pp. 108-111, 1986.

Moeller, C. C., L. E. Gumley, K. I. Strabala, and W. P. Menzel, "High Resolution Depiction Of SST And SSC From MAMS Data". *Fourth Conf. on Satellite Meteorology and Oceanography*, San Diego, CA, pp. 208-212, 1989

_____, W. P. Menzel, and K. I. Strabala, "High Resolution Atmospheric And Surface Variability From Combined MAMS And VAS Radiances." *Topical Meeting on Optical Remote Sensing of the Atmosphere*, Reno, Nevada, 1990.

Rothermel, J., R.M. Hardesty, and R.T. Menzies, "Multi-center Airborne Coherent Atmospheric Wind Sensor," Preprints, *Topical Meeting on Optical Remote Sensing of the Atmosphere*, Salt Lake City, UT, March 8-12, 1993.

Spencer, R.W., R.E. Hood, F.J. LaFontaine, E.A. Smith, R. Platt, J. Galliano, V.L. Griffin, and E. Lobl, "High Resolution Imaging Of Rain Systems With The Advanced Microwave Precipitation Radiometer." *J. Atmos. Oceanic Technol.*, in press, 1994.